Inhibition of the Crystallization in Nanofilms of Poly(3-hydroxybutyrate)

María J. Capitán,* Daniel R. Rueda, and Tiberio A. Ezquerra

Instituto de Estructura de la Materia, CSIC, Serrano 119, Madrid 28006, Spain

Received March 3, 2004; Revised Manuscript Received May 18, 2004

ABSTRACT: The aim of this work is to obtain amorphous thin films of poly(3-hydroxybutyrate) (PHB) at room temperature. The PHB thin films were obtained by spin-coating of chloroform−polymer solutions on glass substrate. The films were extensively characterized by X-ray diffraction and AFM. In this work it has been shown that the local interaction of the polar groups of the polymer with the glass substrate reduces the chain mobility, precluding the crystallization within a tens of nanometers thick region close to the polymer−substrate interface. That makes possible to obtain stable amorphous PHB nanofilms at room temperature, opening a new insight into the technological applications of this polymer. Above this critical film thickness the polymer is able to crystallize, but the polymer chains tends to lie down parallel to the air−polymer interface. This crystal growth anisotropy is reduced with the increasing of the film thickness.

1. Introduction

The increasing concern about the human pollution makes the research on biodegradable and natural polymers of primary interest. Thus, a main aim is to obtain biodegradable polymers with similar properties to those offered nowadays by other standard nonbiodegradable polymers. Poly(3-hydroxybutyrate) (PHB) is a natural and biodegradable polyester found in some bacteria as an energy storage system as small granules within the cell.[1] Because of biosynthesis, PHB is a highly chiral polymer with a relative low glass transition temperature (around 5 °C). Thus, PHB reaches a high degree of crystallization with very large spherullites at room temperature when it is isolated from the bacteria.[2] But the high degree of crystallinity makes it opaque and brittle, hampering its wide applicability as biodegradable plastic.[3,4] It is a remarkable feature of PHB that although the isolated polymer is highly crystalline, the native PHB within the cell granules are found only in the amorphous state.[5] Thus, bacteria can more easily obtain the stored energy upon polymer digestion.

In 1992, Calvert[5] described the existing controversy to explain the amorphous character of PHB in vivo. The first necessary step is to understand the mechanism which inhibits the crystallization process in the bacteria. While Sanders and co-workers[6,7] suggest that some clever biological plasticizing occurs in vivo, de Koning and Lemstra[8] argue that the small granules found in bacteria are simply too small to allow the polymer to crystallize in such a small volume because of the low nucleation rate. They estimate from nucleation rate data[3] that the crystallization time for a granule of 0.5 μm diameter is over 30 000 years at 20 °C. The preparation of artificial small granules of PHB[9,10] provided experimental support for the nucleation rate hypothesis against the plasticizing theory.

To obtain PHB in the amorphous state at room temperature is a technological challenge because of its mechanical properties. Furthermore, PHB is also interesting for its optical activity due to the presence of chiral site in the D- (or R-) configuration in its monomer. This fact implies that films and solutions of PHB will induce a rotation of the polarized plane as light passes through envisioning attractive optical applications of this biopolymer.[11] However, for optical applications, the existence of a crystalline phase which scatters light is certainly a huge drawback. Thus, the aim of this work is to obtain amorphous nanofilms of PHB. It is known that the confinement of polymers in ultrathin films affects strongly several physical properties including glass transition temperature,[12] molecular mobility,[13] and crystallization[14−16] among others. In particular, the crystallization growth rate in polymer ultrathin films was shown to decrease with decreasing film thickness.[15,16] This effect has been attributed to a reduction in molecular mobility.[15] Assuming that the nucleation rate is the only factor which affects the crystallization,[8] in a coated film of 2 cm × 2 cm in area and 10 nm thick around 15 min after deposition should appear to be crystalline. Accordingly, it seems impossible to obtain thin films of amorphous PHB, hampering the technological goals. However, we will show, in this paper, that nanofilms of PHB, prepared by spin-coating, are amorphous still after several months. We consider that the main reason for the amorphous nature of the PHB thin films (within tens of nanometers thick), coated on glass substrate, is a local interaction of chain segments inhibiting their crystallization ability.

2. Experimental Methods

2.1. Sample Preparation. PHB of molecular weight M_w = 710 000 g/mol was supplied by PHB Industrial, Brazil.[17] The industrial production of PHB uses the bacteria *Alcaligenis eutrophus* grown on butyric acid/fructose, so getting a highly stereoregular polymer chains. PHB shows a glass transition temperature about 5 °C and a melting temperature around 175 °C similar to that of polypropylene. Chloroform solutions of PHB with different concentrations were used to prepare spin-coating films on cleaned glass surfaces (2.5 cm × 3.0 cm). Solutions from 0.66 up to 83.0 mg/cm^3 were used in the thin films preparation. Samples are labeled by the mother solution concentration. A 0.1 cm^3 volume of polymer solution was added by means of a syringe to the glass surface rotating at about

* Corresponding author: Fax +34 915642431; e-mail capitan@iem.cfmac.csic.es.

10.1021/ma049576p CCC: $27.50
Published on Web 06/25/2004

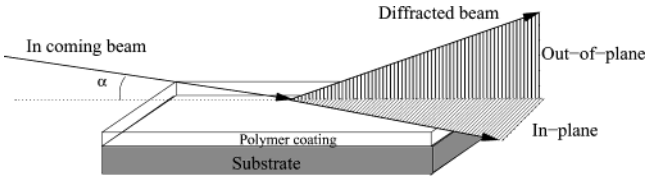

Figure 1. Schema of the X-ray scanning directions with respect to the substrate surface.

1700 rpm. The thinnest coated films samples (concentration < 5 mg/cm^3) did not show any birefringence under optical microscopy.

To compare with the bulk behavior, a micrometer thick PHB film was prepared by evaporation from a concentrated solution (125 mg/cm^3) by evaporation on a glass substrate.

2.2. X-ray Diffraction. The samples were structurally characterized by means of X-ray diffraction using a rotating Cu Kα anode X-ray source. Profiting on the huge versatility that gives the 4 + 2 surface diffraction goniometer[18] placed in the rotating anode, it was possible to study the sample thickness and roughness by means of reflectivity configuration and the polymer structure both perpendicular and parallel to the substrate surface direction by means of wide-angle X-ray scattering experiments with in-plane and out-of-plane configuration, respectively (see Figure 1). The detection was made by using a 0D scintillator monochromatized by using a graphite analyzer. The large dynamic range necessary to avoid the detector saturation on the measured reflectivity was performed by combining the detector with a dynamic automatic filter system described elsewhere.[19]

The X-ray anode station was also equipped with a 2D CCD camera (Princeton Instrument) placed over a 2m length mobile bank along the direct beam axis. The detector has a 65 mm × 65 mm active surface and was occasionally used during this study.

2.3. Atomic Force Microscopy (AFM). AFM images were obtained at room temperature in an AFM DI D3000 Nanoscope IIIA equipment manufactured by Digital Instruments working in tapping mode.

3. Results

The results are presented consecutively, taking into account the increasing thickness of the PHB coating being classed in three ranges of thickness.

3.1. Tens of Nanometers Thick Films (PHB Coating A). The good planarity of these thin films is inferred by the well-defined multiple Kissing peaks in their reflectivity curves[20] (see Figure 2). An estimation of the film thickness is derived from the corresponding Fourier transform analysis based on the Born approximation[21,22] of each curve of Figure 2. The calculated film thickness are 9.1, 12.0, 18.2, 24.1, and 27.0 nm from top to bottom, respectively, in this figure. Thus, the film thickness is directly related to the concentration of the mother solution for the same rotating speed and volume used.

It can be observed a constant intensity region close to the direct beam (Figure 2). In this region, below the critical angle ($\alpha_c = 0.17°$ for PHB), the X-rays are totally externally reflected; i.e., the X-ray wave field in the film is evanescent, and it is limited to the top ≤5 nm of the polymer coating.[23]

The amorphous nature is clearly confirmed by their X-ray diffractograms recorded using the grazing incidence technique (Figure 3, left plot). All the PHB coating A films have a similar amorphous diffraction pattern in both in-plane and out-of plane directions at low incident angle (Figure 3, left plot). The diffraction pattern are characterized by the absence of any Bragg peak (indicating lack of crystalline material) over a very broad bump intensity characteristic of an amorphous material. The polymer contribution is superimposed to the glass substrate signal, indicating that the polymer coating is amorphous.

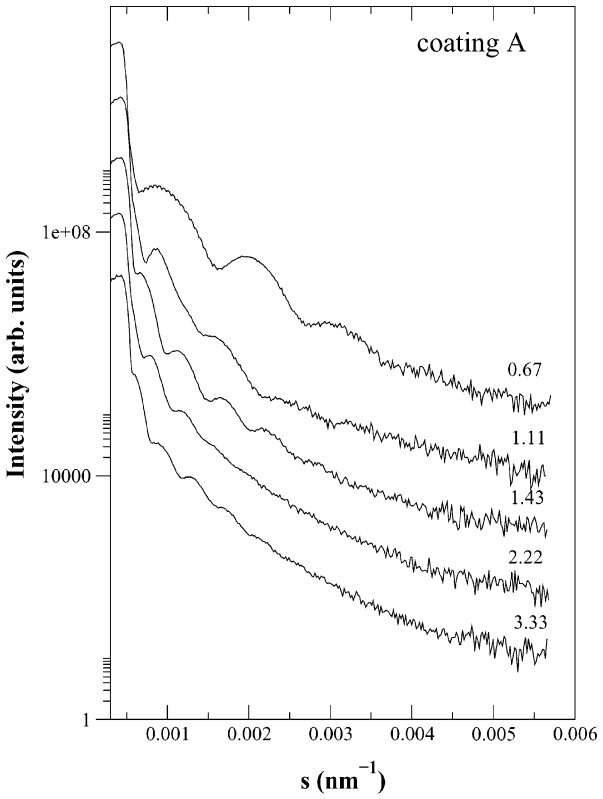

Figure 2. X-ray reflectivity curves of nanofilms of PHB coated on glass surface. The PHB coatings were prepared using different solution concentrations of PHB in chloroform. The concentrations were referred to mg of PHB solved in 1 cm^3 of chloroform volume and are indicated on each trace of the plot. The higher the polymer dilution, the thinner the PHB coating as it is inferred from the larger periodicity of the Kissing peaks. On the *x*-axis is presented the reciprocal vector, *s* ($s = 2 \sin \theta/\lambda$; X-ray wavelength, $\lambda = 0.154\ 18$ nm).

3.2. Hundreds of Nanometers Thick Films (PHB Coating B). For the medium thickness spin-coating films investigated the main feature is the almost lack of Kissing peaks close up to the direct beam (Figure 4, upper line) but where it still remains the total reflection region with a high intensity. This behavior corresponds to a slightly rougher interface (polymer−air interface) in this film. The film thickness (170 nm thick) was estimated by means of ellipsometry techniques comparing with previous films with a well-known thickness by reflectometry. It is important to point out that for this medium thickness film the reflectivity diagram presents also a broad small-angle scattering peak ($s \approx 0.002$ nm^{-1}) that corresponds to a correlation distance of 4.7 nm. This distance is sensitively too small with respect to the film thickness, and its origin should be discussed later on. At wide-angle scattering (see middle plot Figure 3), it is worth noticing the presence of only a crystalline peak (at 13.4°) in the out-of-plane scan whose intensity remains almost constant for all diffractograms recorded at different incidence angles. The peak position corresponds to the 020 Bragg peak of the orthorhombic structure characteristic of the crystalline PHB.[24] The presence of this unique Bragg peak along the direction perpendicular to the surface (out-of-plane) indicates a preferential crystallization of the PHB with the *ac* plane

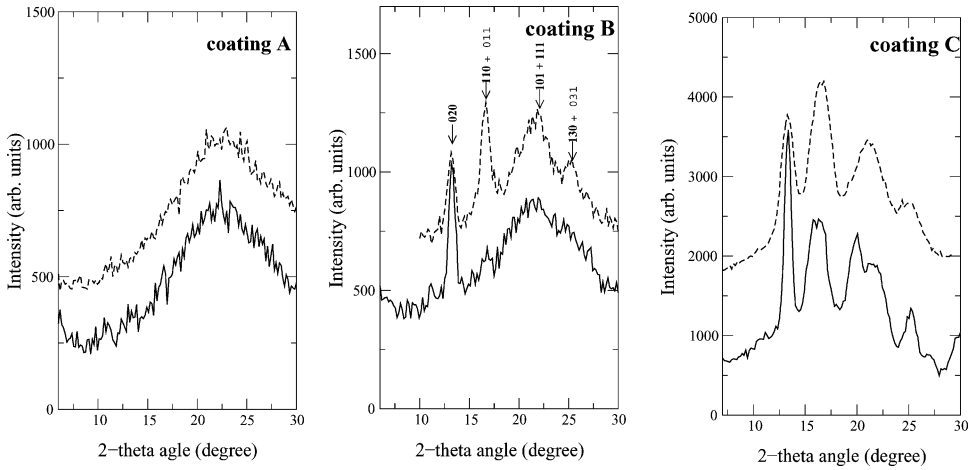

Figure 3. X-ray diffractograms of the PHB films coated on glass surface for the three representative thickness class: coating A (left), coating B (middle), and coating C (right). The diffractograms presented here were recorded using a grazing incidence angle of 0.4° in both out-of plane (continuous line) and in-plane scattering directions. Left and middle figures are for spin-coating PHB films (27.0 and 170 nm thick) prepared using solution concentrations of 3.33 and 83.33 mg/cm^3, respectively. Right figure is for a coated PHB film (18 μm thick) prepared by slow evaporation of a concentrated solution (125 mg/cm^3). Notice the amorphous nature of the thinner nanofilm (left) and the preferential crystallization (middle) observed for the coating 170 nm thick.

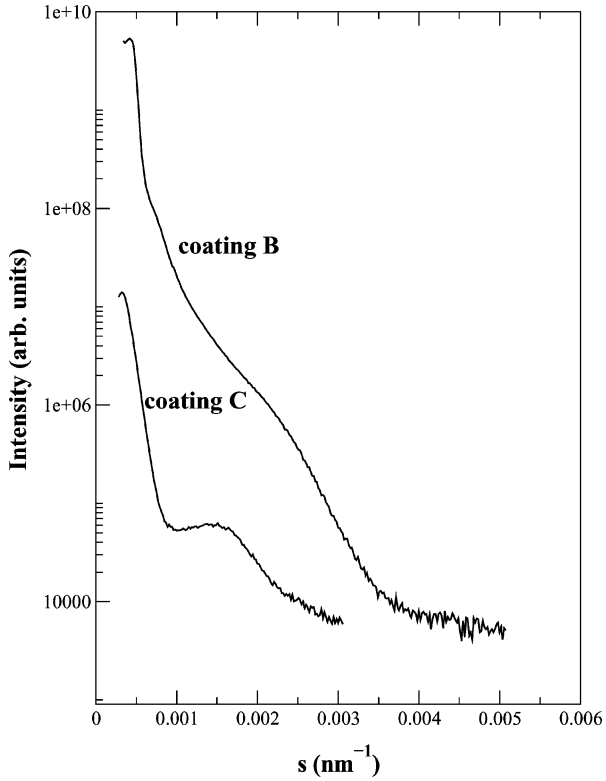

Figure 4. Small-angle X-ray scattering curves of the two thickest PHB films: upper curve, spin-coating film of ≈170 nm thick; lower curve, cast film of 18 μm thick.

parallel to the surface. This point is confirmed in the in-plane scan (dashed line in Figure 3, middle plot) where the main Bragg peak became the 110. Thus, the polymer chain lies parallel to the substrate surface. Furthermore, a coherent crystal size of about 15 nm is derived from the fwhm of the 020 peak.

3.3. Micrometer Thick Films (PHB Coating C). In the upper limit, micrometer thick samples were prepared over the glass substrate by solution-cast films of PHB, after evaporation of chloroform. They appear to be semicrystalline according to their X-ray pattern (Figure 3, right plot) which is similar to that reported for bulk PHB.[9,24] However, it is observed a relatively high intensity of the 020 Bragg peak along the direction perpendicular to the surface compared to a nonoriented powder. The relative Bragg peak intensity is changed when it is recorded in the in-plane direction, becoming the 110 Bragg peak the main one (Figure 3, right plot). This fact indicates that even in this thick sample the presence of air interface influences the crystal orientation.

The thick film (18 μm) obtained from solution-cast shows small-angle X-ray scattering curve with a well-resolved broad peak (Figure 4, lower line). From peak position, a distance periodicity of 6.4 nm is derived. This value is close to but lower than that reported for PHB membranes[25,26] and that observed for melt crystallized PHB[3,27] and corresponds to distances in the polymer of around 7.0−8.0 nm.

3.4. Morphology of PHB Coating As Revealed by AFM. Figures 5−7 show the AFM tapping mode pictures for the amplitude and phase for the three reprensentative PHB coatings recorded at differents spatial resolution. In accordance with the X-ray results, the AFM image of the thinnest coating type A samples exhibit a structureless picture (Figure 5). It is remarkable the morphology observed for the B coating (about 170 nm thick). The surface is covered by large polygonal entities (about 2 μm radius) resembling the spherulitic structure. The absence of crystallinity in the very thin films (coating A) indicates that it must be a region of about 30 nm thick close to the substrate−polymer interface where the polymer crystallization is precluded. Taking into account the small crystallized thickness (≤140 nm) and the large dimension of polygons (24 times higher), they are almost 2-dimensional entities in contrast to the 3-D character of spherulites; they are named thereafter as "2D spherulites". 2D spherulites seem to have grown from a center, and their surface is marked by plenty of circular dots like smallpox on the skin.

The AFM images of higher resolution (Figure 5b) clearly show a nice lamellae structure morphology developed for both two PHB coating clearly visualized as white stripes. The excellent contrast obtained between the crystalline lamellae and the amorphous phase is due to the fact that the AFM images were taken at

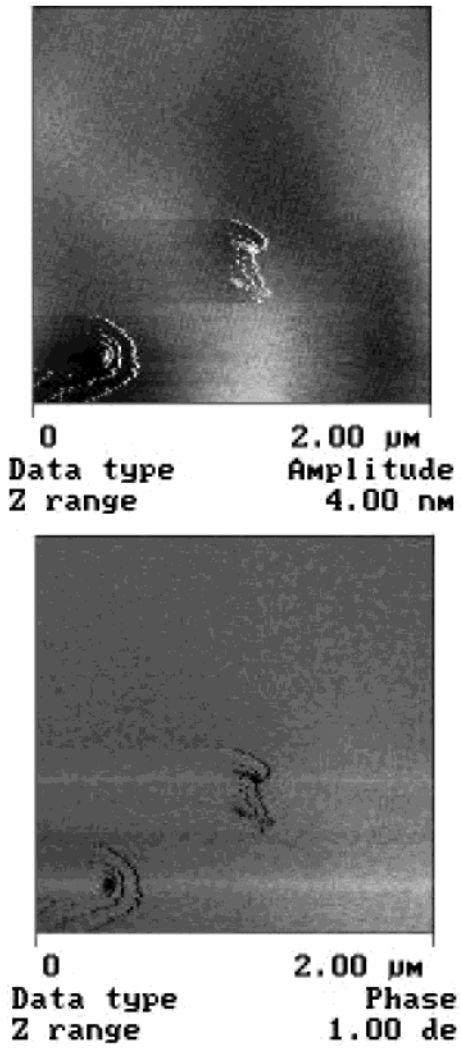

Figure 5. AFM images of the PHB A coating film at 2 μm magnification. This samples exhibits a structureless picture.

room temperature which is well above the glass transition temperature of PHB. This condition has been shown as crucial in order to obtain high-resolution images in polymer crystallization experiments.[28] Nevertheless, main differences in the lamellae wide values and their distribution in wide can be observed between the two samples. Thus, for the B coating the lamellae wideness distribution is narrower and much thinner throughout the surface than those observed for the C coating. Furthermore, taking into account the high axial orientation in the B coating sample observed by X-ray diffraction, it can be assigned its texture to the fact that most of lamellae are edge-on disposed on the polymer−air interface in this sample. Such orientation tends to be also preferable in the case of the solution cast film (C coating).

4. Discussion

4.1. Structural Anisotropy Induced by the Coating Thickness. It have been shown that the deposition of the PHB polymer over a glass substrate appears to be different depending on the coating thickness. While at low covering thickness the crystallization is inhibited, at medium and high film thickness crystallinity appears although with some crystal anisotropy. The crystallites tends to be oriented with the polymer chains parallel to the substrate surface. This preferential orientation

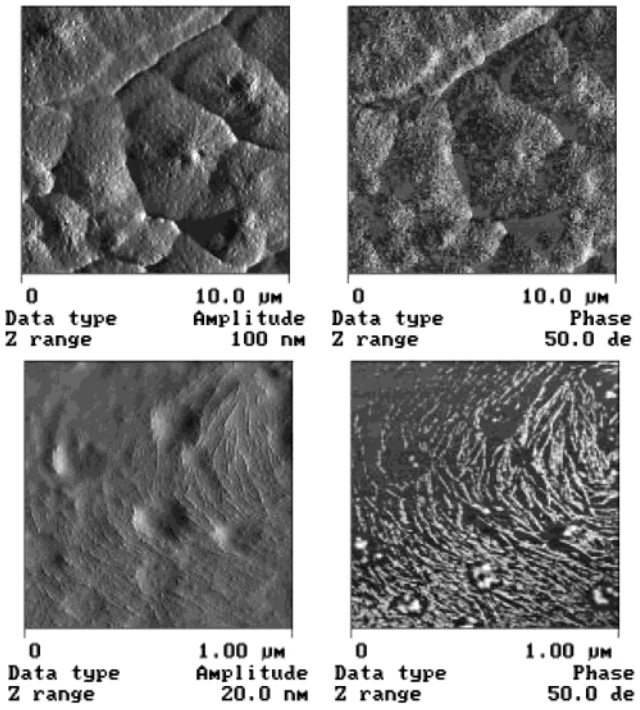

Figure 6. AFM images of the PHB coating B sample at (up) 10 μm and (down) 1 μm magnification. It can be observed at the higher magnification that it is clearly appreciable the intergrain boundaries in this sample (similar to the spherullites shape observed by optical microscopy). In the high magnification it can be observed the a very homogeneous thickness in the lamellae structure.

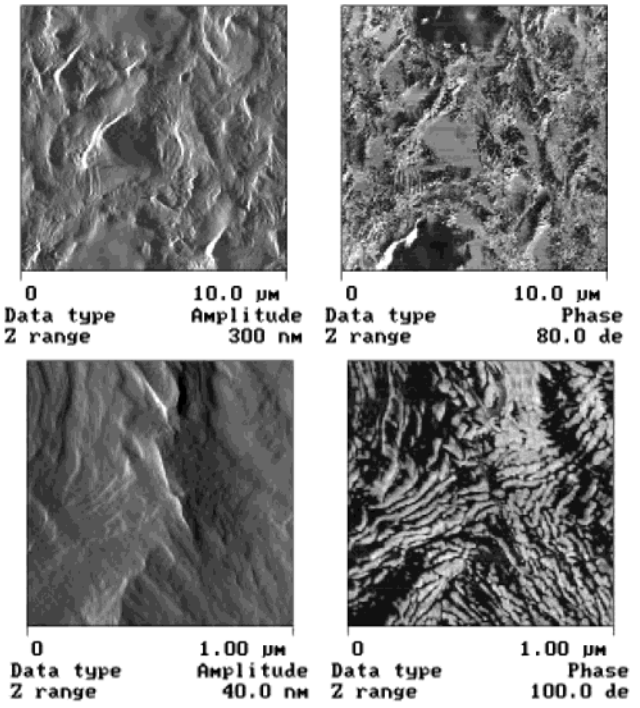

Figure 7. AFM images of the PHB coating C film (up) 10 μm and (down) 1 μm magnification. It can be observed that this sample has a more rough surface compared with previous ones. The lamellae structure observed in the higher magnification is less homogeneous than for the coating B film.

is more dramatic in the coating B sample. This film only presents the 020 Bragg peak in the out-of-plane diagrams (continuous line in Figure 3, middle), being the

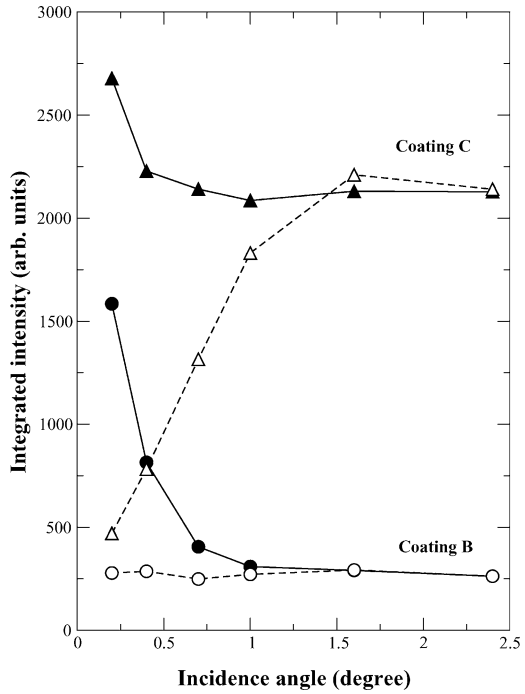

Figure 8. Intensity variation of the Bragg peak at 13.4° with the grazing incidence angle. The X-ray diffractograms of Figure 3 have been analyzed by measuring, particularly, the integrated intensity of the peak at 13.4°: data as observed (open symbols) and after correction for the illuminated volume of sample (filled symbols) for the PHB spin-coating 170 nm thick (circles) and for the PHB cast film 18 μm thick (triangles).

110 Bragg peak the main reflection in the in-plane (dashed line).

To determine whether this structural restriction is imposed by the polymer−substrate interface or at the polymer−air one,[23] detailed structural information on the coating in depth was obtained by the analysis of X-ray scattering patterns recorded at different incidence angles. Thus, we have recorded X-ray diffractograms for each PHB coating at consecutive, increasing incidence angle (0.2, 0.4, 0.7, 1.0, 1.6, and 2.4°). We have selected the peak at 13.4°, indexed as 020 for the crystal lattice of PHB,[24] from diffractograms of Figure 3 and measured the integrated intensity of the peak before and after correction for the volume of sample illuminated by X-rays. The variation of peak intensity with the incidence angle, for both B and C PHB coatings, is represented in Figure 8. For the noncorrected diffractograms (open symbols) the peak intensity remains constant with incidence angle in the case of the thinner sample (170 nm) while it increases linearly first and then it levels off at high incidence angle values in the case of the thickest sample (18 μm). The corresponding corrected values of peak intensity (filled symbols) are also shown. The larger intensity values derived for small incidence angles would support a larger crystallinity degree of PHB at the outer surface of the polymer coatings (proximities to the polymer−air interface). The effect of the surface ordering in thin polymer films has been reported in the literature and can be interpreted assuming a layer model.[29] Recent experimental works also support this effect.[30] Furthermore, taking into account the preferential crystal orientation given by the wide-angle diffraction pattern (Figure 3, middle plot), it can be concluded that the *b*-axis of the orthorhombic crystal unit cell of PHB[24] prefers to lie down parallel to the transfer momentum and, thus, perpendicular to the surface.

According to these results, chain segments in the proximities to the polymer−air interface of the PHB coating B crystallize more easily than those segments from inner surfaces, closer to the substrate. This observation is supported by recent views about the dynamic of thin films.[29] Most of the phenomenology about the dependence of the glass transition temperature of a polymer with thickness can be interpreted assuming the layer model[29] which incorporates a mobile surface layer in the polymer−air interface and restricted mobility regions associated with the polymer−substrate interface. The presence of this restricted region close to the polymer−substrate interface makes that the tens of nanometers thick films should be amorphous. In that case the film thickness can be considered comparable to the extent of this restricted region. This crystallization constraint could be related with the presence of polar groups in the PHB which promotes a strong interaction with the glass surface. This kind of polar polymer−glass substrate interaction, which reduces significantly the polymer mobility, has been reported in a great variety of systems either confined in glass pores or deposited onto glass substrate.[15,31]

It is important to note the structural stability of the amorphous PHB films on the glass substrate. After 6 months of sample preparation, the coating A samples not only show reflectivity curves identical to those presented in Figure 2 but X-ray diffractograms revealing that samples still remain amorphous. Concerning the PHB coating B (170 nm) X-ray diffractograms, recorded at different incidence angles, did not change their character at all. This means that the initial, outer crystallization has not continued in depth during storage of sample at room temperature. It is remarkable that previous studies in poly(ethylene oxide) (PEO) have shown crystallization even for very thin films (15 nm), and the polymer/substrate interactions were only responsible for a decrease of the crystal growth rate.[15] However, coating A films with thickness up to 27 nm appear to be completely amorphous even after 6 months of storage at room temperature. This difference between PHB and PEO coatings could be related to the difference between their glass transition temperatures (5 and −78 °C for PHB and PEO, respectively). The reduction in thickness provokes an increase of T_g of about 30 °C for PEO,[15] shifting it to about −40 °C, which is still well below room temperature. Therefore, a similar shift of the T_g for PHB will frozen the polymer chain avoiding any crystallization at room temperature. Nevertheless, a slight perfection or growth of crystallites has occurred as it is inferred from a sharpening of the reflection at 13.4°. Indeed, a reduction of peak breadth (fwhm) of 0.2° was measured (the initial fwhm was of 0.8°).

4.2. Modification of the PHB Microstructure with the Film Thickness. It is remarkable the shift in angular position of the broad SAXS bump (around $\approx$0.002 nm^{-1} in Figure 4) observed between the B and C samples. To explain this fact, it is necessary to discuss about the origin of this signal. On one side, the coating A films, which were amorphous, do not present any bump at this position (Figure 2). For bulk polymers it is well-known that the appearing of such kind of SAXS intensity requires a semicrystalline nature of the sample. Furthermore, the angular position of the SAXS maximum is related to the average intercrystallites distances

or long periodicity (L). In the other side, it was already shown that both B cnd C samples, which presents this SAXS signal, are semicrystalline at room temperature (Figure 3). Thus, it can be related this signal to the film microstructure. However, the L values derived from Figure 4 (4.7 and 6.4 nm for the B and C coating, respectively) are considerably smaller than the value observed from melt-crystallized PHB (about 7.0−8.0 nm).[3,25−27]

In an attempt to shine a light over this missmatch, some atomic force microscopy (AFM) images were recorded. In the high-magnification AFM images (Figure 5b) the crystalline lamellae are clearly visualized as white stripes. The observed stripes thickness are sensitively lower and more homogeneous in the coating B sample than in C. This fact together with the higher axial orientation of sample B given by the wide-angle X-ray data (Figure 3) indicates that for the coating B film most of the crystallite lamellae appear in edge-on orientation while for the coating C a wider orientation distribution should be present although with a significant prevail of edge-on lamellae orientation. Assuming that the interlamellae distance may change with the crystallite axis, then the observed relatively low correlation length, and its decreasing with the film thinness can be related to an increasing of the crystal anisotropy from C to B samples. Thus, the high anisotropy in the B film could be a plausible origin of the so low correlation distance derived from SAXS signal.

In thin films the appearance of X-ray signal at low diffraction angle can also be due to the formation of an outermost layer film of different density.[32] The AFM images and the film reflectivity show a film roughness higher (of about hundreds of nanometers as derived from the z-scale) than the measured correlation length associated with the SAXS bump in Figure 4 (lower than 7.0 nm). Thus, in our case the formation of an outermost layer of lower density due to the film roughness can be discarded as origin of the SAXS signal. Other authors[33] relate the appearance of a low correlation distance signal in low crystallized samples to the formation of blocks crystallize within self-assembling microdomains rather than forming laterally extended lamellae domains. These authors observed such microdomains in the AFM images. In our case, the AFM images of the B film present also a granular structure homogeneously distributed but its size (≈200 nm) is 40 times bigger than the corresponding to the SAXS signal. Thus, the AFM images allow to discard also case this origin. A dependence of the crystallite size with the film thickness could also be in the origin of the observed too low correlation distance. Therefore, we consider that the high orientation anisotropy induced by the low thickness of PHB coating film is the more plausible origin of the low correlation distance derived from SAXS. However, it cannot be discarded that the SAXS signal shift comes from the different critical size of the crystallites in the films reached at the equilibrium.

5. Final Remarks and Conclusions

We have shown that there is two extreme regions from the crystallization point of view in PHB thin films. First, a region in the proximities of the substrate−polymer interface in which the polymer chain suffer a strong constraint to crystallize likely produced by the interaction of the polar groups of PHB with those of the glass substrate. Second, a region in the proximities to the polymer−air interface in which the polymer is able to crystallize provided a minimum thickness of coating. Thus, depending on the film thickness, one can obtain either amorphous PHB films, for thickness in the tens of nanometers range, or semicrystalline PHB films of thickness above hundreds of nanometers range. In this last case, it has been shown that the polymer chains tends to lie down parallel to the polymer−air interface. While this characteristic preferred orientation is preserved at the outer face, it is progressively reduced toward the core of a thick coating. For a 170 nm thick film (B coating) the polymer−air surface is formed by groups of crystal lamellae with 2D spherulites shape (about 4 μm of diameter) impinging each other.

We have demonstrated that PHB can be directly prepared as stable, amorphous films coated on a glass surface. The findings reported here, obviously, open new and interesting perspectives for technological applications of this biodegradable and optically active[11] polymer where the mechanical and optical properties provided by an amorphous film are required. The important point is that such a possibility is now obtained for a biodegradable polymer material.

Acknowledgment. The authors thank MCYT, Spain, Grants FPA-2001-2139 and BFM2001-0174 and CAM, Spain, Grant 07N/0023/2002 for the financial support. Authors thank Mr. W. M. Pachekowski for handing over us the PHB material and Dr. G. Broza and Prof. K. Schulte for allowing us the use of the AFM microscope at the TU Hamburg-Harburg and Dr. R. Serna for performing the ellipsometry measurements.

References and Notes

(1) Lageveen, R. G.; Huisman, G. W.; Preusting, H.; Ketelaar, P.; Eggink, G.; Witholt, B. *Appl. Environ. Mocrobiol.* **1988**, *54*, 2924−2932.
(2) Barham, P. J. *J. Mater. Sci.* **1984**, *19*, 3826−3834.
(3) Barham, P. J.; Keller, A.; Otun, E. L.; Holmes, P. A. *J. Mater. Sci.* **1984**, *19*, 2781−2794.
(4) Anderson, A. J.; Dawes, E. A. *Microbiol. Rev.* **1990**, *54*, 450−472.
(5) Calvert, P. *Nature (London)* **1992**, *360*, 535−535.
(6) Amor, S. R.; Rayment, T.; Sanders, J. K. *Macromolecules* **1991**, *24*, 4583−4588.
(7) Harrison, S. T. L.; Chase, H. A.; Amor, S. R.; Sanders, J. K. M. *Int. J. Biol. Macromol.* **1992**, *14*, 50−56.
(8) de Koning, G. J. M.; Lemstra, P. J. *Polymer* **1992**, *33*, 3292−3294.
(9) Horowitz, D. M.; Clauss, J.; Hunter, B. K.; Sanders, J. K. M. *Nature (London)* **1993**, *363*, 23−23.
(10) Horowitz, D. M.; Sanders, J. K. M. *J. Am. Chem. Soc.* **1994**, *116*, 2695−2702.
(11) Holmes, P. A. *Phys. Technol.* **1985**, *16*, 32−36.
(12) Keddie, J. L.; Jones, R. A. L.; Cory, R. A. *Europhys. Lett.* **1994**, *27*, 59−64.
(13) Frank, B.; Gast, A. P.; Russell, T. P.; Brown, H. R.; Hawker, C. *Macromolecules* **1996**, *29*, 6531−6534.
(14) Reiter, G.; Sommer, J.-U. *Phys. Rev. Lett.* **1998**, *80*, 3771−3774.
(15) Schönherr, H.; Frank, C. W. *Macromolecules* **2003**, *36*, 1199−1208.
(16) Despotopoulou, M. M.; Frank, C. W.; Miller, R. D.; Rabolt, J. F. *Macromolecules* **1996**, *29*, 5797−5804.
(17) Nascimento, J. F. *Disertaçao de mestrado*; UNICAMP, Dpto. de Engenheria Quimica, Campinas, 2001.
(18) Vlieg, E.; van der Veen, J. F.; Gurman, S. J.; Norris, C.; MacDonald, J. P. *Surf. Sci.* **1989**, *210*, 301−321.
(19) Alvarez, J.; Paiser, E.; Capitán, M. J. *Rev. Sci. Instrum.* **2002**, *73*, 2788−2790.
(20) Als-Nielsen, J. X-ray reflectivity studies in liquid surfaces. In *Handbook of Synchrotron Radiation*; Brown, G., Moncton, D. E., Eds.; North-Holland: Amsterdam, 1991; Vol. 3, pp 471−504.
(21) Bridou, F.; Pardo, B. *J. Phys. III* **1994**, *4*, 1523−1531.

(22) Li, M.; Muller, M. O.; Landwehr, G. *J. Appl. Phys.* **1996**, *80*, 2788−2790.
(23) Toney, M. F.; et al. *Nature (London)* **1995**, *374*, 709−710.
(24) Yokuchi, M.; Chatani, Y.; Tadokoro, H.; Teranishi, K.; Tani, H. *Polymer* **1973**, *14*, 267−272.
(25) Krivandin, A. V.; Shatalova, O. V.; Iordanskii, A. L. *Vysokomolek. Soedin., Ser. A and B* **1997**, *39*, 1865−1868.
(26) Factor, B. J.; Russell, T. P.; Toney, M. F. *Macromolecules* **1993**, *26*, 2847−2859.
(27) Rule, R. J.; Liggat, J. J. *Polymer* **1995**, *36*, 3831−3840.
(28) Ivanov, D. A.; Amolou, Z.; Magonov, S. N. *Macromolecules* **2001**, *34*, 8944−8952.
(29) Fonest, J. A.; Mattsson, J. *Phys. Rev. E* **2000**, *61*, R53−R56.
(30) Durell, M.; Macdonald, J. E.; Trolley, D.; Wehrum, A.; Jukes, P. C.; Jones, R. A. L.; Walker, C. J.; Brown, C. *Europhys. Lett.* **2002**, *58*, 844−850.
(31) Schüller, J.; Richert, R.; Fischer, E. W. *Phys. Rev. B* **1995**, *52*, 15232−15238.
(32) Gautam, K. S.; Kumar, S.; Wermeille, D.; Robinson, D.; Dhingwala, A. *Phys. Rev. Lett.* **2003**, *90*, 215501.
(33) Loo, Y. L.; Register, R. A. *Phys. Rev. Lett.* **2000**, *84*, 4120−4123.

MA049576P